J|A|C|S COMMUNICATIONS

Published on Web 12/23/2008

Anisotropic Electron Transport Properties in Sumanene Crystal

Toru Amaya,[†] Shu Seki,*[,†] Toshiyuki Moriuchi,[†] Kana Nakamoto,[†] Takuto Nakata,[†] Hiroyuki Sakane,[†] Akinori Saeki,[‡] Seiichi Tagawa,[‡] and Toshikazu Hirao*[,†]

Department of Applied Chemistry, Graduate School of Engineering, Osaka University, Yamada-oka, Suita, Osaka 565-0871, Japan, and The Institute of Scientific and Industrial Research, Osaka University, Mihogaoka, Ibaraki, Osaka 567-0047, Japan

Received July 31, 2008; E-mail: hirao@chem.eng.osaka-u.ac.jp; seki@chem.eng.osaka-u.ac.jp

Polyaromatic carbon molecules including fullerenes and carbon nanotubes have been attracting great interest because of their promising potential for electrical materials.[1] In this context, bowl-shaped polyaromatic hydrocarbons or π-bowls are now considered to be another group of key materials in the science of nonplanar π-conjugated carbon systems. The synthesis, structural characterization, and complexation of π-bowls have been actively investigated for about 15 years.[2] However, the research on molecular electronics has not been performed with π-bowls so far. We have studied the C_{3v} fullerene fragment π-bowl "sumanene" (**1**, $C_{21}H_{12}$) since the first synthesis in 2003 (Figure 1a).[3,4] X-ray crystallographic structure analysis of **1** showed the 1D columnar π-stacking in a concave−convex fashion, where every column is present in the same direction.[4a] Each layer is stapled with a staggered fashion probably due to a repulsive effect of the three methylene units and/or maximization of the HOMO−LUMO overlap. These properties motivated us to investigate the potential utility as electrically active materials in a solid state. Here, we report the charge carrier mobility of the needle-like crystal of **1** using time-resolved microwave conductivity (TRMC) method, which shows the large intracolumnar electron mobility (7.5×10^{-1} cm^2 V^{-1} s^{-1}) and its remarkable anisotropy (9.2 times) along the π-bowl stacking column axis.

The charge mobility of organic materials is quantified by direct current methods, such as time-of-flight (TOF) and field-effect transistor (FET) methods. In these methods, the mobility is strongly influenced by various factors, such as a quite small amount of impurity, chemical and physical defects, organic/electrode interfaces, due to a long distance carrier transportation from the contact electrode. On the other hand, the TRMC method can minimize such factors because the nanometer-scale mobility of charge carriers generated by laser pulse irradiation is quantified under oscillating microwave without electrodes.[5] In this study, the TRMC method was employed to examine the intrinsic carrier mobility of **1**.

The needle-like single crystal of **1** (approximate dimensions $280 \times 200 \times 700$ μm^3) was prepared from hexane/CH_2Cl_2 solution. This crystal is stable under air. The crystalline indices are shown in Figure 1b.[6] The crystal is a hexagonal cylinder. X-ray crystal structure analysis of this crystal confirmed a 1D columnar stacking structure as reported before.[4a,7] This stacking structure contrasts markedly with that of a planar polyaromatic hydrocarbon like triphenylene.[8] Staggered stacking is depicted in green and yellow in Figure 1c. It should be noted that the crystallographic *c* axis (the [001] direction) is parallel to the long axis of this needle-like crystal (Figure 1b).

Figure 2a shows the conductivity transient observed for the needle-like single crystal of **1**. The single crystal (approximate dimensions $250 \times 250 \times 1000$ μm^3) was set in a microwave cavity whose standing electric field direction was parallel or perpendicular to the π-bowl stacking axis of the crystal to estimate the transient conductivity of the photogenerated charge carriers along the respective directions. The maximum value of $\phi\Sigma\mu$ reaches 4.5 ×

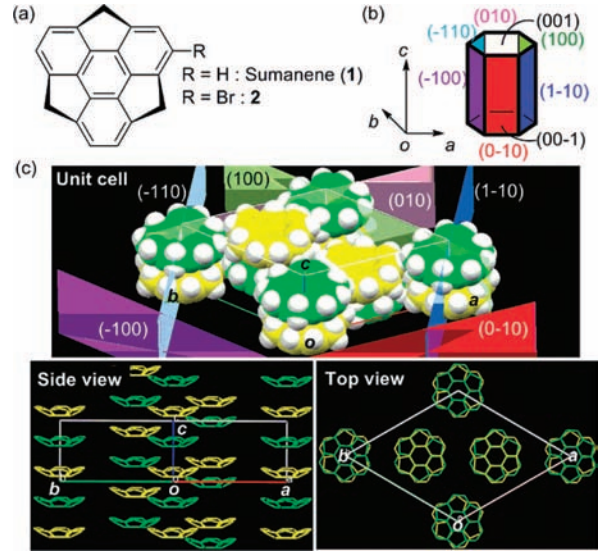

Figure 1. (a) Sumanene (**1**) and Br-sumanene **2**; (b) the crystalline indices of a needle-like crystal of **1**; (c) a packing structure of a needle-like crystal of **1**. A staggered stacking is depicted in green and yellow. Hydrogen atoms are omitted in the side and top views for clarity.

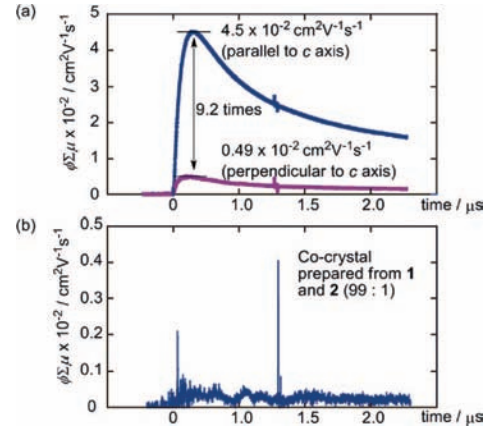

Figure 2. (a) Conductivity transients observed for a single crystal of **1**. Blue and violet lines are the transients observed along the directions parallel and perpendicular to the stacking axis (*c* axis) of the crystal, respectively. The transients were recorded under an excitation at 355 nm, 0.83 mJcm^{-2}. (b) The transient observed for a cocrystal prepared from **1** and **2** (99: 1) under the same excitation conditions.

[†] Graduate School of Engineering, Osaka University.
[‡] The Institute of Scientific and Industrial Research, Osaka University.

10.1021/ja805997v CCC: $40.75

10^{-2} cm^2 V^{-1} s^{-1} along the π-bowl stacking axis, where ϕ and $\Sigma\mu$ denote photocarrier generation yield (quantum efficiency) and sum of mobilities for positive and negative charge carriers, respectively. On the other hand, the much smaller transient conductivity was exhibited along the perpendicular direction to the π-bowl stacking axis (0.49×10^{-2} cm^2 V^{-1} s^{-1}). The anisotropic difference reaches 9.2 times. This can be explained by efficient $\pi-\pi$ overlap between the layers. Generally, the anisotropy of crystals tends to remain low because of close packed π-conjugated molecules, in contrast with the π-stacked discotic liquid crystal possessing the insulating alkyl chains.[9] The obtained value is higher than that of rubrene single crystal,[5e] and comparable to that of dehydrobenzo[12]annulene single crystal.[10] Charge carrier generation and decay kinetics are also investigated (Supporting Information, Figure S2), giving the risetime of ~50 ns and the apparent initial first-order decay rate constant of 8×10^5 s^{-1}, respectively. The risetime is almost consistent with the time constant of the set of apparatus, suggesting the intercolumnar charge separation (Figures S6 and S8) through the singlet excited-state of **1**.[11] The apparent first-order decay of the conductivity transient is predominantly attributed to the recombination of the carriers with traps and/or impurities.

The dynamics of the charge carriers was also examined using a cocrystal of **1** and the bromo substituted derivative **2** (Figure 1a) to determine the charge carrier species because the high electron affinity of the bromo group is known to give effective negative charge carrier traps. Br-sumanene **2** was synthesized from **1** by treatment with pyridinium hydrobromide perbromide. A cocrystal was prepared from the hexane/CH_2Cl_2 solution of **1** and **2** (99:1). The thus-obtained needle-like cocrystal was analyzed by EI-MS and elemental analysis to show the presence of **2** (Figure S4).[12,13] X-ray crystal structure analysis of this needle-like cocrystal also confirmed a 1D columnar stacking structure as observed with **1**.[14] The photograph is shown in Figure S5 (approximate dimensions $70 \times 70 \times 1400$ μm^3). The corresponding conductivity transient observed for a cocrystal of **1** and **2** is also displayed in Figure 2b. Despite ~2% of the molecules being substituted by the bromo group, the observed conductivity transient resulted in a dramatic drop ($<0.05 \times 10^{-2}$ cm^{2}V^{-1}s^{-1}) in comparison with that of the single crystal of **1**. This could be explained by the trapping of electrons by the bromo group, leading to dissociation of the Br-aromatic bond.[15] These findings suggest that the major charge carrier is electrons in the π-stacking structure.

To confirm the charge carrier generation yield and species, photocurrent integration measurement was performed on a solid film of **1** sandwiched by Au and Al electrodes.[16] Transient photocurrent was observed mainly under the negative bias (3 V, Figure S3), also suggesting electrons as the major charge carrier species. The integration of the transient current gives the maximum yield of photocarrier generation under the applied bias as $\phi \approx 0.06$, which is unusually high as the yield of free charge generation in the conjugated organic crystals because of the high electric field strength in this measurement. Applying the maximum ϕ value in the single crystal of **1**, the minimum estimate of the intracolumnar electron mobility along the π-bowl stacking axis is calculated to be 7.5×10^{-1} cm^2 V^{-1} s^{-1}. This value is comparable to that of a single crystal of C_{60} (0.5 ± 0.2 cm^2 V^{-1} s^{-1} measured by TOF),[17] one of the representative compounds showing n-type OFET properties. The observed high electron mobility of **1** might be attributed to the curved π-conjugated system. On the basis of this mobility and one period of 9.1 GHz microwave field (110 ps), the displacement length of mobile electron along the stacking is calculated to be approximately 20 nm corresponding to 52 sumanene molecules. Accordingly, ~2% of Br-sumanene **2** is considered reasonable to trap an electron.

In conclusion, the needle-like single crystal of **1** was revealed to show the high electron mobility with large anisotropy by the TRMC method. These findings allow the development of electrical materials such as OFET based on π-bowls.

Acknowledgment. This work was financially supported in part by a Grant-in-Aid for Young Scientists (B) from Japan Society for the Promotion of Science and collaborative development of innovative seeds, potentiality verification stage from Japan Science and Technology Agency (JST).

Supporting Information Available: Experimental details, spectral data for **2**. This material is available free of charge via the Internet at http://pubs.acs.org.

References

(1) (a) Baxendale, M. Carbon nanotubes and bucky materials. In *Springer Handbook of Electronic and Photonic Materials*; Kasap, S., Capper, P., Eds.; Springer: 2006; Chapter *50*, pp 1147−1154. (b) Anthony, J. E. *Angew. Chem., Int. Ed.* **2008**, *47*, 452.
(2) (a) Rabideau, P. W.; Sygula, A. *Acc. Chem. Res.* **1996**, *29*, 235. (b) Mehta, G.; Rao, H. S. P. *Tetrahedron* **1998**, *54*, 13325. (c) Petrukhina, M. A.; Scott, L. T. *Dalton. Trans.* **2005**, 2969. (d) Wu, Y.-T.; Siegel, J. S. *Chem. Rev.* **2006**, *106*, 4843. (e) Tsefrikas, V. M.; Scott, L. T. *Chem. Rev.* **2006**, *106*, 4868.
(3) Sakurai, H.; Daiko, T.; Hirao, T. *Science* **2003**, *301*, 1878.
(4) (a) Sakurai, H.; Daiko, T.; Sakane, H.; Amaya, T.; Hirao, T. *J. Am. Chem. Soc.* **2005**, *127*, 11580. (b) Amaya, T.; Mori, K.; Wu, H.-L.; Ishida, S.; Nakamura, J.; Murata, K.; Hirao, T. *Chem. Commun.* **2007**, 1902. (c) Amaya, T.; Sakane, H.; Hirao, T. *Angew. Chem., Int. Ed.* **2007**, *46*, 8376. (d) Amaya, T.; Sakane, H.; Muneishi, T.; Hirao, T. *Chem. Commun.* **2008**, 765.
(5) (a) Seki, S.; Yoshida, Y.; Tagawa, S.; Asai, K.; Ishigure, K.; Furukawa, K.; Fujiki, M.; Matsumoto, N. *Philos. Mag. B* **1999**, *79*, 1631. (b) Grozema, F. C.; Siebbeles, L. D. A.; Warman, J. M.; Seki, S.; Tagawa, S.; Scherf, U. *Adv. Mater.* **2002**, *14*, 228. (c) Saeki, A.; Seki, S.; Sunagawa, T.; Ushida, K.; Tagawa, S. *Philos. Mag.* **2006**, *86*, 1261. (d) Yamamoto, Y.; Fukushima, T.; Jin, W.; Kosaka, A.; Hara, T.; Nakamura, T.; Saeki, A.; Seki, S.; Tagawa, S.; Aida, T. *Adv. Mater.* **2006**, *18*, 1297. (e) Saeki, A.; Seki, S.; Takenobu, T.; Iwasa, Y.; Tagawa, S. *Adv. Mater.* **2008**, *20*, 920.
(6) The photograph of the needle-like crystal of **1** is shown in Figure S1.
(7) Crystal data for **1**: trigonal, space group *R*3*c* (No. 161), $a = 16.6402(3)$ Å, $c = 7.7024(1)$ Å, $V = 1847.03(6)$ Å^3, $Z = 6$; $R1 = 0.033$; w$R2 = 0.086$. The data have been deposited with the Cambridge Crystallographic Data Centre: CCDC-266603.
(8) (a) Klug, A. *Acta Crystallogr.* **1950**, *3*, 165. (b) Ahmed, F. R.; Trotter, J. *Acta Crystallogr.* **1963**, *16*, 503. (c) Collings, J. C.; Roscoe, K. P.; Thomas, R. L.; Batsanov, A. S.; Stimson, L. M.; Howard, J. A. K.; Marder, T. B. *New J. Chem.* **2001**, *25*, 1410.
(9) (a) van de Craats, A. M.; Warman, J. M.; Müllen, K.; Geerts, Y.; Brand, J. D. *Adv. Mater.* **1998**, *10*, 36. (b) van de Craats, A. M.; Warman, J. M.; Fechtenkötter, A.; Brand, J. D.; Harbison, M. A.; Müllen, K. *Adv. Mater.* **1999**, *11*, 1469. (c) Pisula, W.; Menon, A.; Stepputat, M.; Lieberwirth, I.; Kolb, U.; Tracz, A.; Sirringhaus, H.; Pakula, T.; Müllen, K. *Adv. Mater.* **2005**, *17*, 684.
(10) Hisaki, I.; Sakamoto, Y.; Shigemitsu, H.; Tohnai, N.; Miyata, M.; Seki, S.; Saeki, A.; Tagawa, S. *Chem. Eur. J.* **2008**, *14*, 4178.
(11) Warman, J. M.; Piris, J.; Pisula, W.; Kastler, M.; Wasserfallen, D.; Müllen, K. *J. Am. Chem. Soc.* **2005**, *127*, 14257.
(12) The surface of the needle-like cocrystal was washed with CH_2Cl_2 before EI-MS measurement and elemental analysis.
(13) Elemental analysis showed approximately 2% inclusion of **2** (Anal. Calcd for $C_{21}H_{12}/C_{21}H_{11}Br = 98/2$: C, 94.89; H, 4.54; Br, 0.57%. Found: C, 95.42; H, 4.58; Br, 0.57%).
(14) Crystal data for a cocrystal prepared from the solution of **1** and **2** (99:1): trigonal, space group *R*3*c* (No. 161), $a = 16.6391(3)$ Å, $c = 7.7027(1)$ Å, $V = 1846.87(6)$ Å^3, $Z = 6$; $R1 = 0.035$; w$R2 = 0.085$. The data have been deposited with the Cambridge Crystallographic Data Centre: CCDC-706689.
(15) (a) Toriyama, K.; Iwasaki, M. *J. Phys. Chem.* **1972**, *76*, 1824. (b) Dusen, W. V., Jr.; Hamill, W. H. *J. Am. Chem. Soc.* **1962**, *84*, 3648. (c) Dillard, J. G. *Chem. Rev.* **1973**, *73*, 589. (d) Irie, M.; Shimizu, M.; Yoshida, H. *J. Phys. Chem.* **1976**, *80*, 2008.
(16) Absorption spectra of **1** in solution and solid film are shown in Figure S7.
(17) Frankevich, E.; Maruyama, Y.; Ogata, H. *Chem. Phys. Lett.* **1993**, *214*, 39.

JA805997V